CHARACTERIZATION AND OPTIMIZATION OF HYBRID CARBON-GLASS EPOXY COMPOSITES UNDER COMBINED LOADING

V. Infante[a], J.F. Aguilar Madeira[a,b], Rui B. Ruben[c,1], F. Moleiro[a], Sofia Teixeira de Freitas[d]

[a] LAETA, IDMEC, Instituto Superior Técnico, Universidade de Lisboa, Av. Rovisco Pais 1, 1049-001 Lisboa, Portugal.
[b] Department of Mathematics, ISEL, IPL, Rua Conselheiro Emídio Navarro, 1949-014 Lisboa, Portugal
[c] CDRsp - ESTG - Polytechnic Institute of Leiria, Campus 2 Morro do Lena – Alto do Vieiro, 2411-901 Leiria, Portugal.
E-mail: rui.ruben@ipleiria.pt
[d] Faculty of Aerospace Engineering, Delft Univ. of Technology, Kluyverweg 1, Delft, Netherlands.

ABSTRACT

This work is intended to characterize the mechanical behavior of hybrid carbon-glass composites plates under combined loading of bending and torsion, and to determine the optimal ply fiber orientations to minimize the maximum out of plane displacement under such loading conditions. Hybrid composite plates were manufactured with 10 plies each and different stacking sequences using hand lay-up, with carbon fiber and glass fiber reinforcements in an epoxy matrix. Two experimental setups (involving two distinct boundary conditions) are here considered to test the composite plates, both simulating combine loading of bending and torsion. Numerical simulations of the experimental tests were performed in ABAQUS® and validated with the experimental data. Using the ply fiber orientations as design variables, the hybrid composite plates were then optimized using GLODS – Global and Local Optimization using Direct Search. The objective function of minimization the maximum out of plane displacement is carried out through an interactive cycle between GLODS and ABAQUS®. Specimens of three optimized laminates were also manufactured for experimental validation. The optimization process contributed to improve the performance of the hybrid composites plates in more than 30% when compared to some non-optimized plates.

[1] Corresponding autor. Address: ESTG - Polytechnic Institute of Leiria, Campus 2 Morro do Lena – Alto do Vieiro, 2411-901 Leiria, Portugal. Tel: +351 244830010. Email: rui.ruben@ipleiria.pt

KEYWORDS:

A. Hybrid composites

B. Carbon and Glass fibers

C. Finite element analysis

D. Optimization

1. INTRODUCTION

Polymer matrix composites are becoming increasingly important in high technology applications, particularly in the aeronautical industry. Aircraft designers typically look for high specific stiffness, high specific strength, low density and reduced cost while selecting the material systems for different structural components. However, due to their characteristic high stiffness and strength, most of the composite materials, using single material reinforcements, have limited toughness values.

Hybrid composites may offer an effective solution for increasing the toughness of a composite material. By combining two fiber types in a single composite, one can take advantage of both fiber properties and try to minimize some of their disadvantages. The hybrid composites concept consist in combining fibers with high modulus and high specific strength, relatively brittle and generally expensive, with fibers with low modulus and lower specific strength, more ductile and frequently cheaper. Carbon fiber laminates are widely used in several applications due to their high specific modulus and strength. Nonetheless, the impact strength of these composites is generally lower than many metal alloys. Previous research has shown that an efficient method of increasing the tensile ultimate strain [1], impact properties [2] as well as flexural strength properties [3, 4] of carbon fiber composites is to add some percentage of low modulus fibers, such as glass fibers, both using intra- or inter- ply hybridization. With this hybridization, the carbon fiber can still provide the necessary stiffness, while the final composite material is cheaper and more damage tolerant due to the presence of the glass fibers. The final mechanical properties of the hybrid composite can be tailored by changing the stacking sequence of the plies (interply hybrid composites – different fiber materials along the stacking sequence) and the volume fraction of each fiber (intraply hybrid composite – different fiber material inside the plies) [5].

The impact performance of interply hybrid composites has been extensively reported by several works found in literature which concluded that hybrid carbon-glass epoxy composites show an

improvement in damage tolerance and carrying capacity after impact in comparison with carbon/epoxy laminates with slight reduction of stiffness [2, 6–8]. Gonzalez et al. (2014) [9] further demonstrates that the stacking sequence of the carbon-glass hybrid composites has a significant influence on the failure mechanisms sequence, growth and interactions during impact tests and compression after impact tests.

Under bending conditions, literature suggests that the best flexural properties of hybrid glass-carbon laminates are obtained when the carbon plies are positioned at the exterior [10]. The same study concludes that the tensile strength was insensitive to the relative position of the glass-carbon plies and an alternate glass-carbon stacking sequence favours compressive strength. Dong et al. [3, 4] tested hybrid laminates under three point bending and observed that the highest flexural strength is achieved when specimens contain 24% of glass fibers. These hybrid laminates show an increase of 8% and 3% when compared to the ones with full carbon and glass configurations, respectively. Simulation studies show much higher increases in flexural strength than the corresponding experiments. When looking to intraply hybrid laminates, literature shows that the fiber volume fraction has a significant influence on the flexural strength. Dong et al. [11] claims that in general in order to improve flexural strength, the fiber volume fraction of glass/epoxy plies needs to be higher than that of carbon/epoxy plies [12]. Few studies were found in which an optimization of the stacking sequence was performed. Kalantari et al. [13, 14] run multiobjective optimization analysis with several objectives such as flexural strength, weight and costs. The results suggest that the hybridization of carbon fiber reinforced composites with glass fibers, and vice versa, not only improves the flexural strength but can also optimize the weight and cost of the composite structure.

Hybrid laminates can also be used for health monitoring purposes, for example. Loading the hybrid composite in the fiber direction in tension, will cause the more brittle fibers to fail before the more ductile fibers. Also, in a laminate with only carbon fiber reinforcements, the replacement of the middle plies by cheaper glass fibers can significantly reduce its cost, while the flexural properties remain almost unaffected [15]. The extensive work performed on characterizing the properties of fiber hybridization under tensile, flexural and impact loading is reported in the comprehensive review of Swolfs et al. [15].

Optimization of composite materials in the field of design of ply orientation has drawn extensive attention over the past two decades [16]. In literature, for example, Todoroki et al. [17] use the Genetic Algorithm (GA) to optimize ply orientation by considering the enforcement constraints to limit the

number of continuous orientation plies. Toropov et al. [18] applied GA to optimize the weight and manufacturability of composite aircraft components. Zhu et al. [19] applied GA to a multiobjective linear variable weights to optimize the stacking sequence and ply thickness of carbon fiber composite struts. The advantage of using such heuristic algorithms is that there is no need to derive design sensitivity information and also the possibility of converging to a global optimum. Another class of methods that does not need any gradient information, but rather require only the value of the objective function, are the direct search methods [20]. The Direct MultiSearch (DMS) [21] is a direct search method for multiobjective optimization. In fact, it has been recently used by Araujo et al. [22] to find the optimal positioning of surface bonded sensors and actuators for damping maximization. It has also been used to solve the problem of minimum weight and maximum damping of viscoelastic sandwich plates by Madeira et al. [23, 24] and to the design optimization of laminated composite plates with piezoelectric layers by Franco Correia et al. [25], among other applications. Global and Local Optimization using Direct Search (GLODS) is a direct search method designed to deal with global optimization problems with a single objective function. This method has been used previously by Monte et al. [26] to optimize the carbon fibers orientation of composite plates in order to minimize their global out of plane displacement. The optimization process has been validated with experimental results. In this paper GLODS is used to optimize a hybrid composite plate under combined loading of bending and torsion.

The works found in literature up to now on hybrid composites, focus on their characterization and optimization under one single loading, such as isolated tensile, or isolated compression or isolated bending. Nevertheless, in real composite structures such loading conditions are rare and a combine loading is often more realistic. For instance, the combined loading of bending and torsion that often occurs in wing skins of an aircraft. Therefore, it is considered essential for their applicability, to investigate the properties of hybrid composites under combined loading of bending and torsion. This paper aims exactly to fill in this gap of knowledge in the current state of the art and go one step further by optimizing the hybrid composite stacking sequence for combined loading conditions.

The main objective of this study is therefore to characterize the mechanical behavior of hybrid composites plates under combined loading of bending and torsion, as well as, to determine the optimal ply fiber orientations to minimize the maximum out of plane displacement under this loading condition.

2. MATERIALS AND SPECIMENS

The two fiber types used in hybrid composites are typically referred to as low elongation (LE) and high elongation (HE) fibers [15]. In the present work, the LE and HE fibers are HS carbon fibers and E-glass fibers, respectively, and these can be combined in many different configurations. The different non-optimized specimens here analysed were produced using the most common ply fiber orientations of 0º and 90º with different stacking sequences.

The specimens were produced using the T700S carbon and E-glass reinforcements in an epoxy matrix resin. The matrix properties are presented in Table 1, in agreement with the supplier (Sicomin®) Technical Datasheet. Specifications for the fabrics and filaments used as reinforcements are presented in Table 2. And in Table 3, the fiber volume fraction of hybrid composites and ply and laminate thickness were presented.

Table 1. Matrix components and properties.

Epoxy resin SR 1500 + Curing agent SD 2503	
Young's Modulus [GPa]	2.86
Tensile Strength [MPa]	71
Density [g/cm^3]	1.00
Poisson's Ratio	0.3

Table 2. Mechanical and acoustic properties of the specimens.

Property	HS Carbon	E-Glass
Type of fabric	T700S	12.600
Fabric aerial weight [g/m^2]	225	600
Filament diameter [μm]	7	17
Filament maximum elongation	2.1%	4.8%
Filament Young's modulus [GPa]	230	74
Filament tensile strength [MPa]	4900	2500
Filament density [g/cm^3]	1.80	2.54
Filament Poisson's ratio	0.25	0.3

Table 3. Fiber volume fraction of hybrid composites and ply and laminate thickness.

Parameter	Values
Thickness of a carbon layer	0.24 mm
Thickness of a glass layer	0.43 mm
Total specimen thickness	3.16 mm
Carbon density	0.5071
Glass fraction	0.5860

Five hybrid composite plates were produced with unidirectional dry fibers using the hand lay-up (HLU) technique. The mixing ratio by weight of the resin and the fibers was 100:33, as recommended by the resin manufacturer.

The curing process consisted in two phases. Initially, each specimen was placed inside a vacuum bag with breather assemblies. Air was extracted from the material using a vacuum pump, and cure occurred at a controlled room temperature of 20 ºC. This vacuum bagging process consolidates the plies and significantly reduces voids in the composite material. After 24 hours in room temperature, each specimen went through a secondary post-cure, during which the specimen is kept inside a furnace for 8 hours at 60 ºC. Five specimens with 10 plies were produced. The number of plies and fiber orientations of each specimen, P1 to P5, are presented in Table 4.

Table 4. Material stacking sequences and ply fiber orientations of specimens made with carbon fiber (C) and glass fiber (G) reinforcements.

Specimen	Number of plies	Material stacking sequence	Ply fiber orientations
P1	10	$[C_3/G_2]_s$	$[0_3/90_2]_s$
P2			$[0_2/90_2/0]_s$
P3			$[0_4/90]_s$
P4			$[0_2/90_3]_s$
P5			$[0/90/0/90_2]_s$

These plies of either carbon fiber or glass fiber reinforced polymer composites may be considered transversely isotropic materials, as a result of their microscopic heterogeneity. It is therefore necessary to identify at least five independent elastic properties to characterize the behavior of the homogenized composite plies [27]. One of the main difficulties encountered in the computation simulation of the hybrid composites is the determination of these properties for each specimen ply materials. To calculate the elastic properties it was first necessary to find the fiber volume ratio for each of them. Hence, two additional specimens were produced, one with only carbon fiber and another with only glass fiber plies both orientated at 0º. The total mass of the plies was measured before starting the hand-lay-up and both composites were weighted after the post-cure process to calculate the fiber volume ratio for the carbon fiber and for the glass fiber composites. The fiber volume ratios obtained for the carbon fiber and glass fiber were the following: v_{cf}= 0.5071 and v_{gf}= 0.5860.

With the fiber volume ratios for each material and the data of Table 1 and Table 2, it was finally possible to calculate the elastic properties for each specimen material layer, with the numerical method proposed and developed by J. M. Guedes et al. [28]: PREMAT. This finite element model is based on a homogenization theory, which assumes that the composite material is locally formed by the spatial repetition of very small microstructures called Representative Elementary Volumes or RVE. Theoretically, it is mechanically admissible to use the elastic properties given by the periodic

homogenization theory of this model, due to the relative dimensions of the filament diameter compared to the thickness of each ply [29]. The elastic properties, obtained using this method, are presented in Table 5. The material strength of each ply used in the failure analysis was also obtained by the homogenization theory [28] (table 5).

Table 5. Properties of ply materials.

Ply material property		Carbon Fiber	Glass fiber
Longitudinal tensile modulus	E11	117.84 GPa	44.49 GPa
Transverse tensile modulus	E22	9.73 GPa	11.34 GPa
In-plane Poisson ratio	ν_{12}	0.27	0.30
Transverse Poisson ratio	ν_{23}	0.25	0.23
In-plane shear modulus	$G_{12}= G_{13}$	3.34 GPa	3.89 GPa
Transverse Shear modulus	G_{23}	2.40 GPa	2.78 GPa
Longitudinal tensile strength	X_T	2231 MPa	1100 MPa
Longitudinal Compressive strength	X_C	1082 MPa	675 MPa
Transverse tensile strength	Y_T	29 MPa	35 MPa
Transverse compressive strength	Y_C	100 MPa	120 MPa
In-plane shear strength	S12=S13	60 MPa	80 MPa
Transverse shear strength	S23	32 MPa	46 MPa

3. EXPERIMENTAL METHODS

Two types of experimental tests were performed, and deformations were measured for each specimen, subjected to bending-torsion loading. The constraints and the loading location in each experimental setup test are illustrated in Figure 1.

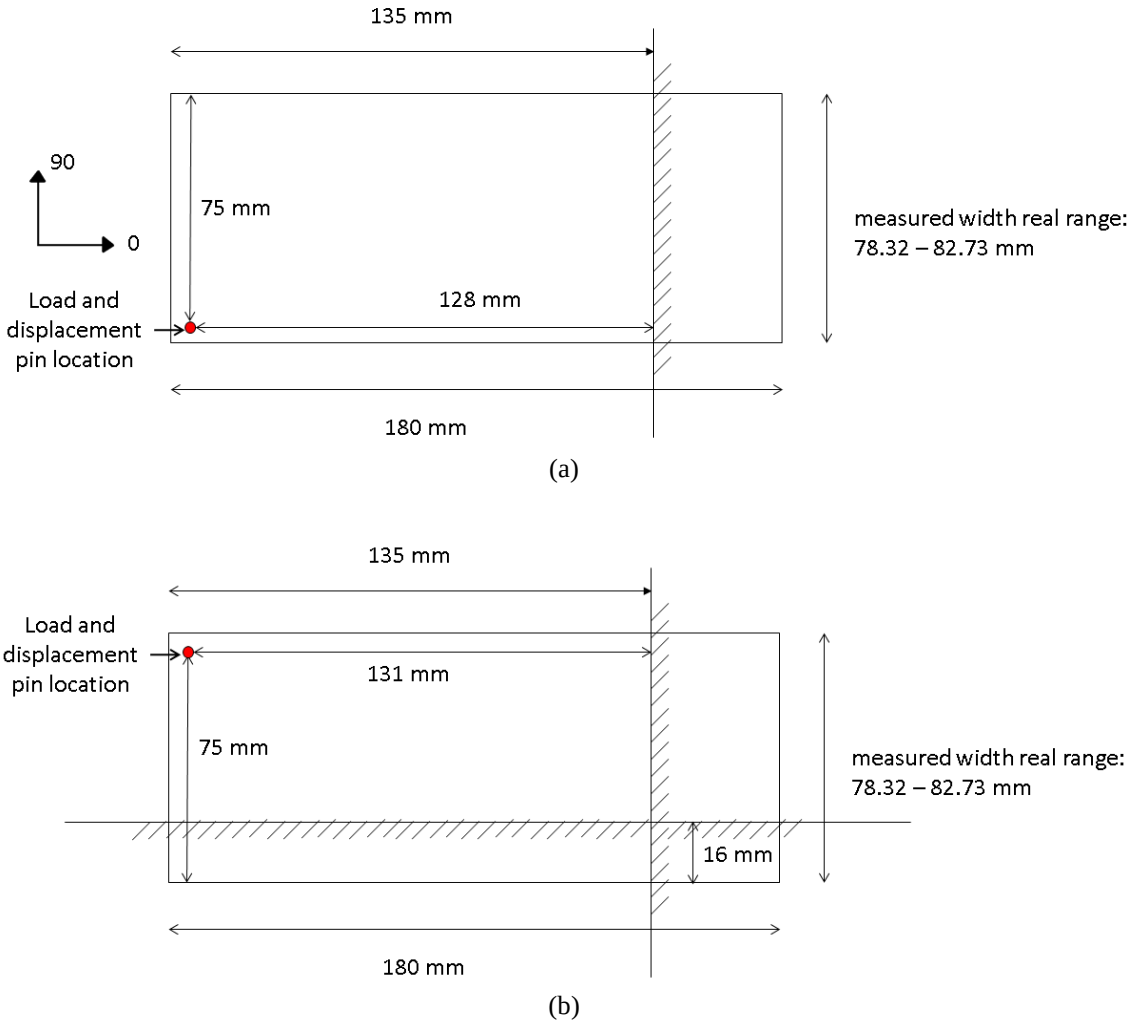

Figure 1. Illustration of the conducted experimental setup tests: (a) plate fixed in one side, (b) plate fixed in two sides.

The experimental tests were conducted in Delft Aerospace Structures and Materials Laboratory (DASML) at Delft University of Technology. Loading occurs at a rate of 2 *mm*/*min* and out of plane displacements are registered using a mechanical clip gauge in the vertical direction of the load location. A picture of each experimental setup is shown in Figure 2.

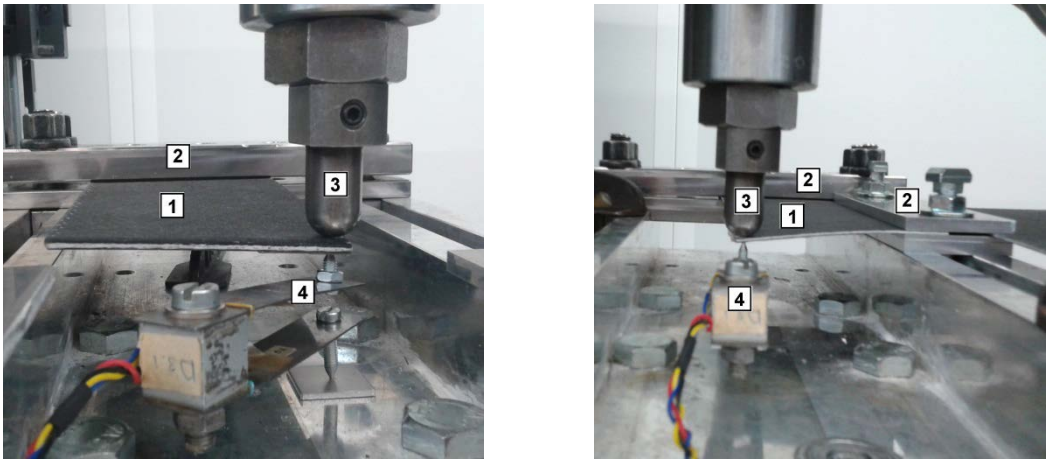

(a) (b)

Figure 2. Experimental bending-torsion tests with the hybrid composite plates: (a) one side fixed; (b) two sides fixed. 1 – Plate; 2 – Fixed side; 3 – Load application; 4 – Mechanical clip gauge.

3.1 Experimental Results

The experimental results are presented in Table 6. The out of plane displacement values were taken at the pin located in the corner of the specimen (applied load location – see Figure 1) for a loading of 50N. This load has been selected to ensure that the specimen is kept within the linear elastic range and prior to any damage initiation. .

Table 6. Out of plane displacements obtained in experimental tests for different loading values.

Specimen	Material stacking sequence	Ply fiber orientations	Experimental test	Loading [N]	Experimental displacement [mm]
P1	$[C_3/G_2]_s$	$[0_3/90_2]_s$	One side fixed	50	3.71
P2		$[0_2/90_2/0]_s$			3.89
P3		$[0_4/90]_s$			3.49
P4		$[0_2/90_3]_s$			4.40
P5		$[0/90/0/90_2]_s$			4.33
P1	$[C_3/G_2]_s$	$[0_3/90_2]_s$	Two sides fixed	50	1.69
P2		$[0_2/90_2/0]_s$			1.37
P3		$[0_4/90]_s$			2.40
P4		$[0_2/90_3]_s$			1.26
P5		$[0/90/0/90_2]_s$			1.16

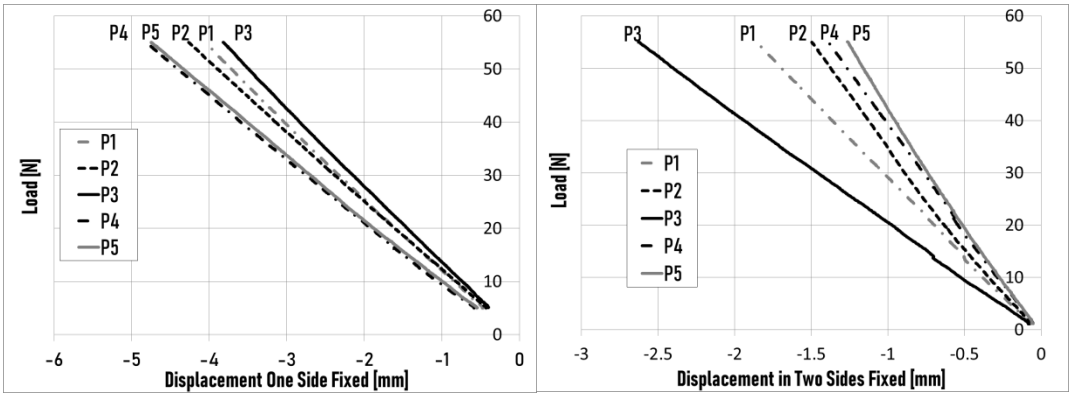

Figure 3. Load-displacement results obtained in the experimental tests.

With the coordinate system of Figure 1 and the data in Table 4, the influence of the fiber orientation of the plies is first analyzed, since all specimens have the same material distribution. By comparing the slope of the graphs in Figure 3, it can be observed that the number of plies at 0º and 90º fiber orientations in each specimen is extremely important for the displacement values. It can be easily seen that for the one side fixed experimental tests the most requested fibers are at 0º, whereas in the experimental test with two sides fixed, the most requested fibers are at 90º.

4. NUMERICAL SIMULATIONS BY FINITE ELEMENT ANALYSIS

A parametric finite element model of hybrid composite plates was developed using ABAQUS®. With the developed parametric model, it is possible to analyze plates with different plies orientation. This parametric model is very useful for the optimization process. In the finite element analysis (FEA) all five plates presented in Table 4 were numerically simulated, in order to validate the numerical results with the experimental out of plane displacements presented in Table 6. A failure analysis was performed based on the FEA results using Hashin's failure criteria [30, 31] for all plates, in order to ensure that the 50 N load is within the linear elastic domain and prior to any damage initiation.

Plies elastic properties considered for the laminates are shown in Table 5, which were obtained with the aforementioned homogenization method. For each experimental setup (one side fixed and two sides fixed), two models were built: one using a 4 node linear shell element (S4), and another one using an 8 node quadratic shell element (S8). A convergence test was done for all 5 plates for both boundary conditions. The P5 plate with one side fixed has the higher displacement value, so also have the slower convergence curve as is showed in Table 7. So, after the convergence test, a significant number of

elements was used to avoid any loss of precision in the optimization method. The same number of elements was used for S4 and S8 shell elements. Specifically, depending on the experimental setup, 3844 and 3224 elements were used, for one side fixed and two sides fixed, respectively. Computational displacement was measured at the load point, as depicted in Figure 4.

Table 7. Convergence test considering P5 with one fixed side.

Number of elements	S4 element		S8 element	
	Computational displacement (mm)	Maximum σ_{11} (MPa)	Computational displacement (mm)	Maximum σ_{11} (MPa)
704	3.93	154.5	3.94	156.8
1344	3.93	154.5	3.94	156.8
1924	3.94	154.5	3.94	156.8
2184	3.94	154.5	3.94	156.8
3244	3.94	154.5	3.94	156.8
3844	3.94	154.5	3.94	156.8
4154	3.94	154.5	3.94	156.8

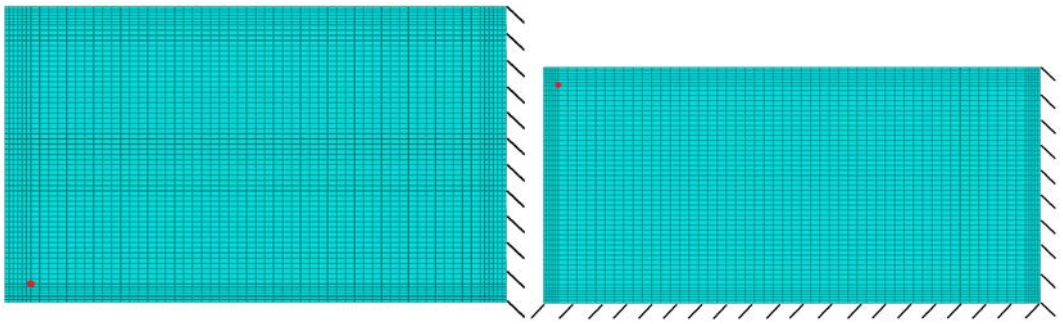

Figure 4. Mesh, boundary conditions, and load/ computational displacement point in red: a) one side fixed; b) two sides fixed.

4.1 FEA Numerical Results

Table 8 presents the out of plane displacements obtained using the FEA as well as the corresponding experimental values. The first immediate observation is that the displacement obtained from the linear and quadratic shell elements models are almost equal. Therefore, the linear 4 node shell element proves to be sufficient for the optimization process while enabling a faster process. Comparing experimental with numerical results, the discrepancy for the one side fixed plates is smaller than for the two sided fixed plates. For all cases, the measured displacement in the experiments is larger than the displacement obtained by FEA. This has also been observed in previous works found in literature, where the flexural stiffness measured in the experiments was lower than the one predicted by the numerical and analytical models [3, 4]. The discrepancy is most probably related with the degree of fixation stiffness at the boundary conditions. In theory, fixed constraints do not allow any displacement or rotation, which is in

fact numerically simulated in the model. However, on the actual experimental test, absolute zero displacements and rotations are very difficult to assure and small displacement and rotations probably occur in fixed sides. Hence, for two sides fixed plates the difference between experimental and computational analysis is naturally higher. In order to better replicate the experimental conditions, fixed constraints that allow infinitesimal rotations were considered (i.e. partially fixed). Boundary conditions were simulated with standard 8 node elements for steel grips. Contrary to fixed conditions, for which there is no gap between steel grips and plate (Figure 5a), for partially fixed conditions, a 5 μm gap is used between top grip and plate, allowing a maximum rotation of 0.1 degrees (Figure 5b). The results of this adapted model are shown in Table 9. As expected, the discrepancy between the model and experiments is now smaller, but some differences still persist. This might be related with the ply properties assumed in the model, which depend on thickness, and the fact that a perfect homogenized ply is almost impossible to manufacture. Figure 6 shows plots of the out of plane displacement field from the FEAs with totally and partially fixed rotation.

Table 8 also presents the results for Hashin's fiber and matrix failure initiation criterion. For both fiber and matrix criteria, table 8 only shows the highest value, which is in all cases the tensile one. As is possible to observe all plates (one sided and two sided fixed) have Hashin's criterion values below 1, which means that no failure occurs.

Table 8. Out of plane displacements and discrepancy percentage between the experimental and the computational analysis using the 4 nodes element.

Specimen	Experimental test	Experimental displacement [mm]	Computational displacement (4 nodes) [mm]	Computational displacement (8 nodes) [mm]	Δ %	Hashin's fiber initiation criterion	Hashin's matrix initiation criterion
P1	One side fixed	3.71	3.12	3.12	15.9	0.0028	0.0233
P2		3.89	3.57	3.56	8.2	0.0038	0.0124
P3		3.49	3.04	3.04	12.9	0.0027	0.0343
P4		4.40	3.58	3.58	18.6	0.0039	0.0123
P5		4.33	3.94	3.94	9.0	0.0048	0.0142
P1	Two sides fixed	1.69	1.43	1.43	15.4	0.0004	0.4655
P2		1.37	0.91	0.91	33.3	0.0002	0.1785
P3		2.40	1.70	1.70	29.2	0.0007	0.6909
P4		1.26	0.91	0.90	28.2	0.0002	0.1741
P5		1.16	0.77	0.77	33.6	0.0002	0.1255

Table 9. Out of plane displacements and discrepancy percentage between the experimental and the computational analysis using partially fixed rotation (instead of totally fixed).

Specimen	Experimental test	Experimental displacement [mm]	Totally fixed [mm]	Partially fixed [mm]	Δ %

P1	One side fixed	3.71	3.12	3.50	5.7
P2		3.89	3.57	3.95	-1.5
P3		3.49	3.04	3.43	1.7
P4		4.40	3.58	3.97	9.8
P5		4.33	3.94	4.32	0.2
P1	Two sides fixed	1.69	1.43	1.67	1.2
P2		1.37	0.91	1.13	17.5
P3		2.40	1.70	1.96	18.3
P4		1.26	0.91	1.12	11.1
P5		1.16	0.77	0.98	15.7

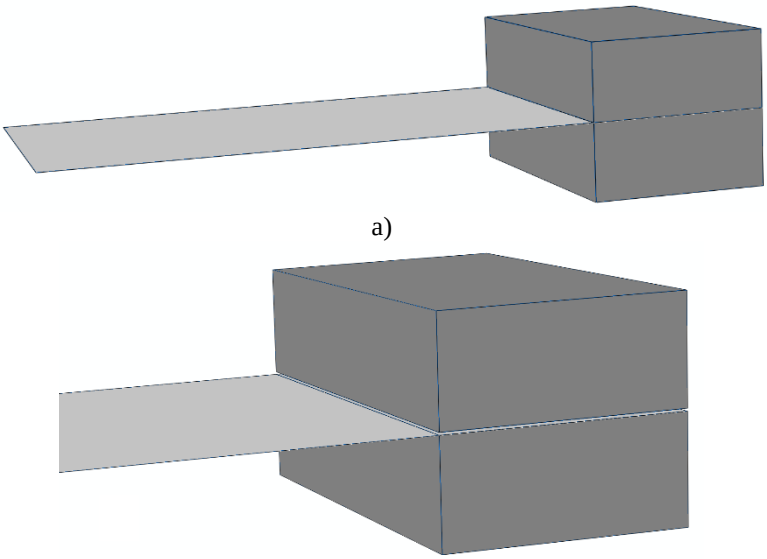

a)

b)

Figure 5. a) One side totally fixed and b) One side partially fixed (gap was increased 100 times for visualization purposes).

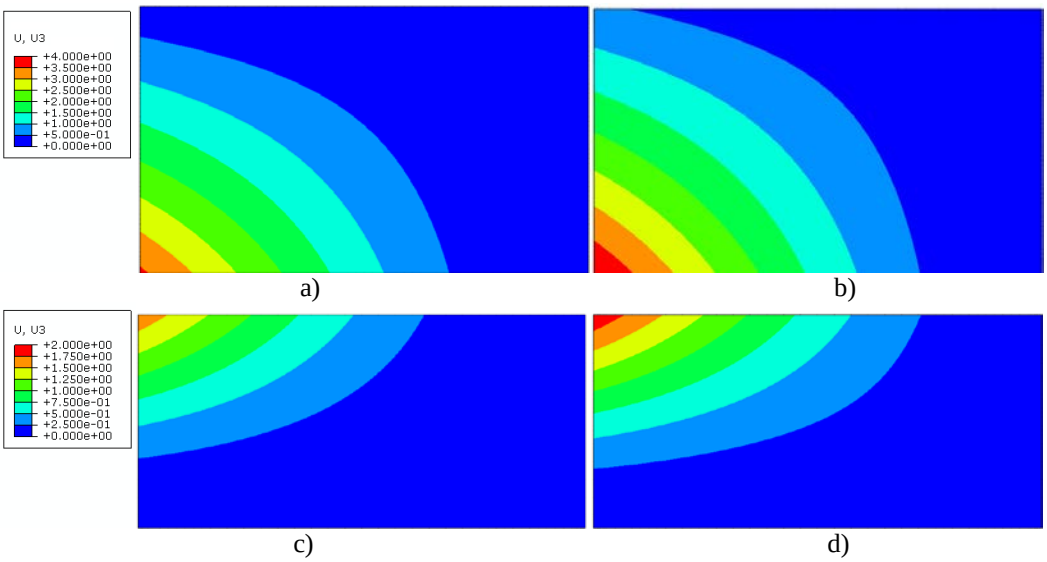

a) b)

c) d)

Figure 6. Displacements in mm: a) and b) P1 with one side fixed; c) and d) P1 with two sides fixed; b) and d) with partially fixed rotations.

5. OPTIMIZATION

The optimization of the specimens was carried out using GLODS, a single objective global optimization method that uses an efficient multistart strategy. The objective function is focused on the minimization of the maximum out of plane displacement value. The objective function evaluation is made through a finite element analysis (FEA) software ABAQUS®. For clarity, a brief introduction to GLODS is given followed by the optimization method used, in order to introduce the optimization problem solved and present the optimal results.

5.1 GLODS (Global and Local Optimization using Direct Search) method

A constrained nonlinear optimization problem can be mathematically formulated as:

Find $\boldsymbol{n}$ design variables:

$$\mathbf{x} = (\boldsymbol{x_1}, \boldsymbol{x_2}, \dots, \boldsymbol{x_n})^{\mathbf{T}} \in \boldsymbol{\Omega} \subseteq \mathbb{R}^{\boldsymbol{n}}, \tag{1}$$

which minimize:

$$\mathbf{min}_{\mathbf{x}\in\boldsymbol{\Omega}}\, \boldsymbol{f}(\mathbf{x}) \tag{2}$$

where $\boldsymbol{f}: \boldsymbol{\Omega} \subseteq \mathbb{R}^{\boldsymbol{n}} \rightarrow \mathbb{R} \cup \{+\infty\}$ represents a real-extended value function and $\boldsymbol{\Omega} \subseteq \mathbb{R}^{\boldsymbol{n}}$ a compact set, defining the problem feasible region.

GLODS [32] is a solver suited for global constrained single optimization, which does not use any derivatives of the objective functions.

Using direct search of directional type, the method alternates between a search step, where potentially good regions are located, and a poll step where the previously located regions are explored. This exploration is made through the launching of several pattern search methods, one in each of the regions of interest. Differently from a multistart strategy, the several pattern search methods will merge when sufficiently close to each other. The goal of GLODS algorithm is to end with as many active pattern searches as the number of local minimizers, which would allow locating easily the possible global extreme value. Similarly to other derivative-free optimization algorithms, it makes use of the extreme barrier function $\boldsymbol{f}_{\boldsymbol{\Omega}}(\mathbf{x})$ defined as:

$$\boldsymbol{f}_{\boldsymbol{\Omega}}(\mathbf{x}) = \begin{cases} \boldsymbol{f}(\mathbf{x}) & \text{if } \mathbf{x} \in \boldsymbol{\Omega} \\ +\infty & \text{otherwise} \end{cases} \tag{3}$$

Unfeasible points will not be evaluated, being the corresponding objective function value set equal to $+\infty$. This approach allows dealing with black-box type constraints, where only a yes/no type of answer is

returned. Several details are omitted in the present text and the reader is referred to Custodio et al. [32] for a more complete description.

5.2 Optimal design formulation

In this work, the objective function is to minimize the maximum out of plane displacement in a composite specimen made with 10 layers with symmetric material stacking sequence $[C_3/G_2]_s$, where C stands for carbon fiber and G for glass fiber. The evaluation of the objective function is made through a finite element analysis (FEA) software, ABAQUS®.

The design variables are the angles of the fiber orientation of 5 plies of the symmetric stacking sequence $[C_3/G_2]_s$ indicated as:

$$\mathbf{x} = (x_1, x_2, x_3, x_4, x_5)^{\mathrm{T}} \tag{4}$$

These angles are discrete variables with allowable variation of 5° in the domain

$$-85° \leq x_i \leq 90°, i = 1, \dots, 5 \tag{5}$$

In the optimization process the default parameters of GLODS are used and the local minimums are found (after 10000 evaluations of the objective function) for each experimental setup: (a) plate fixed in one side, (b) plate fixed in two sides. The optimization carried out considered in the ABAQUS® simulations the theoretical fixed displacement and rotation as boundary conditions (i.e. totally fixed). These optimal results are presented in Table 10 for both experimental setups. The Hashin's failure criteria were also applied to the three optimized stacking sequences. For the optimized plates, the highest value for the Hashin's fiber criterion is 0.0027 for specimen P6 and for the Hashin's matrix criterion is 0.0148 for specimen P8. Both values are bellow one, which means that no failure is expected in the optimized plates for the tested load.

Table 10. Optimal solutions obtained by GLODS for each experimental setup, with two local minima for the case of plate fixed in two sides.

Specimen	Experimental test	Number of plies	Material stacking sequence	Ply fiber orientations	Displacement value [mm]
P6	One side fixed	10	$[C_3/G_2]_s$	[15/15/15/0/15]s	2.130
P7	Two side fixed			[-60/90/-60/60/-45]s	0.358
P8	Two side fixed			$[-60/-60/75/-60/-60]_s$	0.357

6. EXPERIMENTAL VALIDATION OF THE OPTIMIZED LAMINATES

Once the optimized stacking sequence of ply fiber orientations is obtained, it is important to validate the optimization process by performing experimental tests on the proposed optimized solutions. For experimental validation, the three optimized specimens configurations (P6, P7 and P8 of Table 10) obtained in the optimization process were manufactured using the same technique as the previous specimens P1, P2, P3, P4 and P5.

Table 11 presents the experimental and numeric results of the out of plane displacement at the location of the applied load, including the numerical results for both cases of totally and partially fixed rotation boundary conditions.

Table 11. Out of plane displacements results of the optimized specimens P6, P7 and P8.

Specimen	Experimental displacement [mm]	Computational displacement – totally fixed [mm]	Computational displacement – partially fixed [mm]
P6	2.35	2.130	2.420
P7	0.60	0.358	0.576
P8	0.62	0.357	0.582

Figures 7 and 8 compare the out of plane displacement results for the non-optimized specimens (P1, P2, P3, P4 and P5) against the optimized specimens (P6, P7 and P8) considering the one side fixed condition and the two sides fixed condition, respectively.

It is quite clear from Figures 7 and 8 the significant decrease of the out of plane displacement of the optimized specimens found by GLODS, P6, P7 and P8, when compared to the non-optimized specimens, P1, P2, P3, P4 and P5, for both sets of boundary conditions. This decrease in out-of-plane displacement from non-optimized laminates to optimized laminates is in accordance with previous optimization works using GLODS with 100% carbon fiber reinforced laminates under combined loading bending and torsion [26].

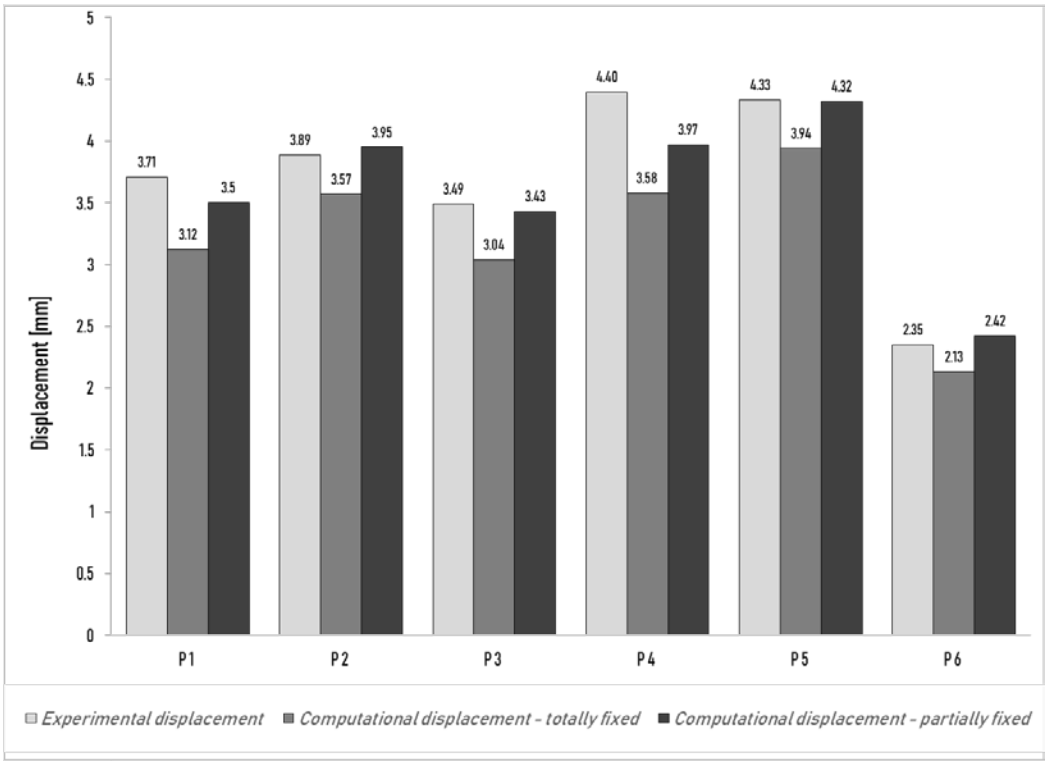

360

361 **Figure 7.** Comparison of experimental and computational values obtained for the non-optimized specimens (P1, P2, P3, P4
362 and P5) and the optimized specimens (P6) considering the plate fixed in one side.
363

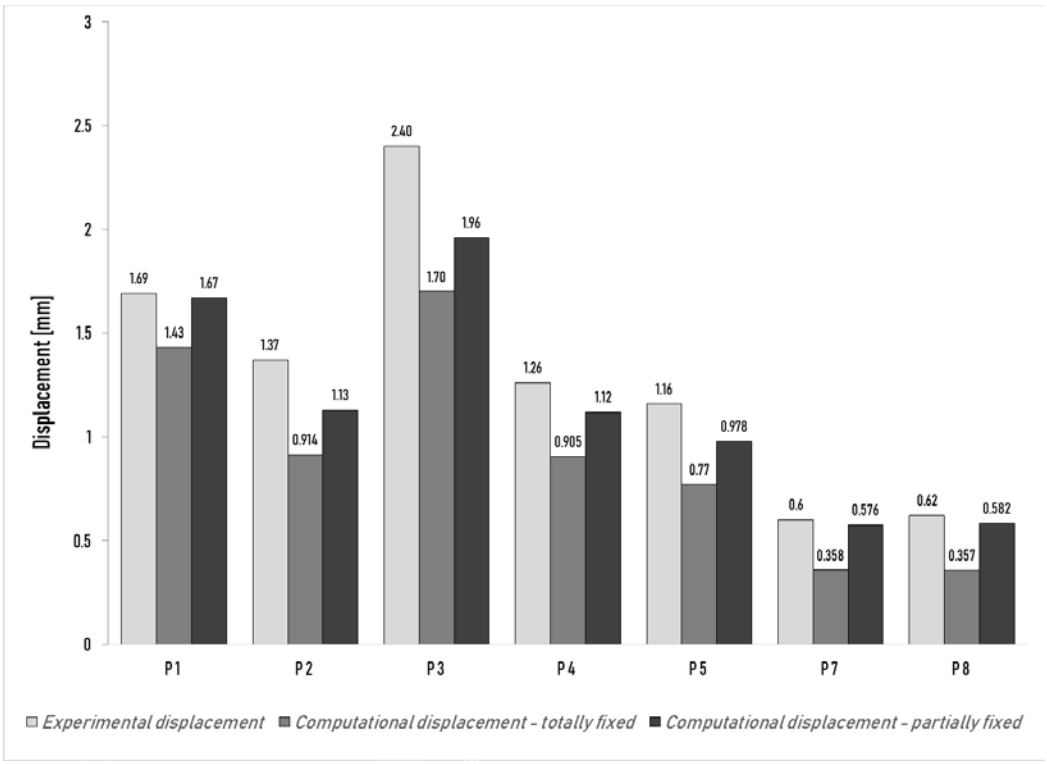

364

365 **Figure 8.** Comparison of experimental and computational values obtained for the non-optimized specimens (P1, P2, P3, P4
366 and P5) and the optimized specimens (P7 and P8) considering the plate fixed in two sides.
367

It is important to recognize that experimental measurements are considered to be the true deformation of the composite specimens, although in reality experimental errors may be inherently present. Specifically, the manufacturing process of each sample may introduce a few unforeseeable imperfections [26, 33], since the laminate quality in Hand Lay-Up is very dependent on the skills of the producer, just as the curing process and the final cutting of the specimen. Meanwhile, the thickness of each carbon fiber ply and each glass fiber ply was calculated with mean values of measurements of the carbon fiber and glass fiber laminates, respectively. Each of the five specimens were measured in 9 points and it was verified that the estimated thickness of the carbon fiber and glass fiber plies had a very good approximation. However, the fact that these values were taken into account in the development of the finite element models may also have contributed to some deviations in the computational results. Additionally, the calculation of the elastic properties of the carbon fiber and glass fiber plies was done by a numerical method based on a homogenization theory. This method depends on the definition of geometric parameters of the Representative Elementary Volume, and as such, it is possible that small errors are associated with these properties relatively to the ply material properties of the specimens tested in the experiments.

The inherent uncertainties altogether, namely, the specimens manufacture using Hand Lay-Up, the real ply material properties and the complexity of replicating numerically the exact boundary conditions placed in the experimental setup tests, naturally introduce some small expected discrepancy between the experimental and computational results. Even so, the optimization process is shown to be quite successful. Not only the computational results of the optimized specimens are validated by the experimental tests (within a reasonable discrepancy), but also the desired improvement of the performance of the hybrid composites plates is achieved in more than 30% when compared to some non-optimized plates. Furthermore, an important aspect that is demonstrated by the optimization of these hybrid carbon-glass epoxy composites is that the most common ply fiber orientations of 0º, 90º and even $\pm 45^{o}$ adopted for various laminated composites applications rather limits somewhat their performance. In a real combined loading condition of bending and torsion, different ply fiber orientations should be explored in the interest of maximizing the hybrid laminated composites performance. This has also been observed for single fiber laminates [26].

7. CONCLUSIONS

The increasing relevance of hybrid carbon-glass epoxy composites, whose mechanical properties can be tailored to take advantage of the better properties of both fiber types, relies on their potential for an increased performance compared to standard composites using one type of fiber alone. The aim of this work was to optimize the hybrid composite stacking sequence, using the ply fiber orientation as design variable to minimize the maximum out of plane displacement under combined loading of bending and torsion. In order to study normal operation conditions, a load within the material linear elastic domain and prior to any damage initiation was considered, as verified throughout the experimental tests and the results from the Hashin's failure criteria.

The optimization process is shown to be quite successful, contributing to improve the performance of the hybrid composites plates in more than 30% when compared to some non-optimized plates. In addition, it is shown that ply fiber orientations different to the most usual 0º, 90º and ±45º should be explored in the interest of maximizing the hybrid laminated composites performance under combine loading of bending and torsion.

CONFLICT OF INTEREST

None.

ACKNOWLEDGEMENTS

This work was supported by "Fundação para a Ciência e a Tecnologia" (FCT), through the Institute of Mechanical Engineering (IDMEC) under the Associated Laboratory for Energy, Transports and Aeronautics (LAETA), Project UID/EMS/50022/2013, and by the Netherlands Organisation for Scientific Research (NWO), project number 14366.

REFERENCES

[1] Pandya KS, Veerraju C, Naik NK. Hybrid composites made of carbon and glass woven fabrics under quasi-static loading. Materials and Design 2011; 32(7): 4094-4099.

[2] Enfedaque A, Molina-Aldareguía JM, Gálvez F, González C, Llorca J. Effect of glass fiber hybridization on the behavior under impact of woven carbon fiber/epoxy laminates. Journal of Composite Materials 2010; 44(25): 3051-3068.

[3] Dong C, Ranaweera-Jayawardena HA, Davies IJ., Flexural properties of hybrid composites reinforced by S-2 glass and T700S carbon fibres. Composites Part B: Engineering 2012; 43(2): 573-581.

[4] Dong C, Davies IJ. Flexural strength of bidirectional hybrid epoxy composites reinforced by E glass and T700S carbon fibres. Composites Part B: Engineering 2015; 72: 65-71.

[5] Kretsis G. A review of the tensile, compressive, flexural and shear properties of hybrid fibre-reinforced plastics. Composites 1987; 18(1): 13-23.

[6] Naik NK, Ramasimha R, Arya H, Prabhu SV, ShamaRao N. Impact response and damage tolerance characteristics of glass-carbon/epoxy hybrid composite plates. Composites Part B: Engineering 2001; 32(7): 565-574.

[7] Hosur MV, Adbullah M, Jeelani S. Studies on the low-velocity impact response of woven hybrid composites. Composite Structures 2005; 67(3): 253-262.

[8] Sayer M, Bektaş NB, Demir E, Çallioğlu H. The effect of temperatures on hybrid composite laminates under impact loading. Composites Part B: Engineering 2012; 43(5): 2152-2160.

[9] González EV, Maimí P, Sainz de Aja JR, Cruz P, Camanho PP. Effects of interply hybridization on the damage resistance and tolerance of composite laminates. Composite Structures 2014; 108(1): 319-331.

[10] Zhang J, Chaisombat K, He S, Wang CH. Hybrid composite laminates reinforced with glass/carbon woven fabrics for lightweight load bearing structures. Materials and Design 2012; 36: 75-80.

[11] Dong C, Davies IJ. Optimal design for the flexural behaviour of glass and carbon fibre reinforced polymer hybrid composites. Materials and Design 2012; 37: 450-457.

[12] Dong C, Davies IJ. Flexural and tensile strengths of unidirectional hybrid epoxy composites reinforced by S-2 glass and T700S carbon fibre. Materials and Design 2014; 54: 955-966.

[13] Kalantari M, Dong C, Davies IJ. Multi-objective analysis for optimal and robust design of unidirectional glass/carbon fibre reinforced hybrid epoxy composites under flexural loading. Composites Part B: Engineering 2016; 84: 130-139.

[14] Kalantari M, Dong C, Davies IJ. Multi-objective robust optimisation of unidirectional carbon/glass fibre reinforced hybrid composites under flexural loading. Composite Structures 2016; 138: 264-275.

[15] Swolfs Y, Gorbatikh L, Verpoest I. Fibre hybridisation in polymer composites: A review. Composites Part A 2014;, 67: 181–200.

[16] Gurdal Z, Haftka RT, Hajela P. Design and Optimization of Laminated Composite Materials. Wiley-Interscience, New York, 1999.

[17] Todoroki A, Haftka RT. Stacking sequence optimization by a genetic algorithm with a new recessive gene like repair strategy. Composites Part B 1998; 29(3): 277–285.

[18] Toropov VV Jones R, Willment, Funnell M. Weight and manufacturability optimization of composite aircraft components based on a genetic algorithm. 6th World Congress of Structural and Multidisciplinary Optimization, Rio de Janeiro, Brazil, 2005.

[19] Zhu X, He R, Lu X, Ling X, Zhu L, Liu B. A optimization technique for the composite strut using genetic algorithms. Materials & Design (1980-2015) 2015; 65: 482–488.

[20] Ghiasi H, Pasini D, Lessard L. Optimum stacking sequence design of composite materials part I: constant stiffness design. Composite Structures 2009;. 90(1): 1–11.

[21] Custodio AL, Madeira JFA, Vaz AIF, Vicente LN. Direct Multisearch for Multiobjective Optimization. SIAM Journal on Optimization 2011; 21(3): 1109–1140.

[22] Araújo AL, Madeira JFA, Mota Soares CM, Mota Soares CA. Optimal design for active damping in sandwich structures using the Direct MultiSearch Method. Composite Structures 2013; 105: 29–34.

[23] Madeira JFA, Araújo AL, Mota Soares CM, Mota Soares CA, Ferreira AJM. Multiobjective design of viscoelastic laminated composite sandwich panels. Composites Part B: Engineering 2015; 77: 391–401.

[24] Madeira JFA, Araújo AL, Mota Soares CM, Mota Soares CA. Multiobjective optimization of viscoelastic laminated sandwich structures using the Direct MultiSearch Method. Composite Structures 2015; 147: 229–235.

[25] Franco Correia VM, Madeira JA, Araújo AL, Mota Soares CM. Multiobjective design optimization of laminated composite plates with piezoelectric layers. Composite Structures 2017; 169: 10–20.

[26] Monte SMC, Infante V, Madeira JFA, Moleiro F. Optimization of fibers orientation in a composite specimen. Mechanics of Advanced Materials and Structures 2017; 24(5): 410-416.

[27] Melro AR, Camanho PP Pinho ST. Influence of geometrical parameters on the elastic response of unidirectional composite materials. Composite Structures 2012;., 94(11): 3223–3231.

[28] Guedes J, Kikuchi N. Preprocessing and postprocessing for materials based on the homogenization method with adaptive finite element methods. Computer Methods in Applied Mechanics and Engineering 1990; 83(2) 143–198.

[29] Coelho PG, Amiano LD, Guedes JM, Rodrigues HC. Scale-size effects analysis of optimal periodic material microstructures designed by the inverse homogenization method. Computers & Structures 2015; 174: 21-32.

[30] Hashin Z. Failure Criteria for Unidirectional Fiber Composites. Journal of Applied Mechanics 1980; 47: 329 334.

[31] Kress G. Examination of Hashin's failure criteria for Part B of the second world -wide failure exercise: comparison with test data. Journal of Composite Materials 2013; 47, (6):7867 -891

[32] Custodio AL, Madeira JFA. GLODS: Global and Local Optimization using Direct Search. Journal of Global Optimization 2015; 62 (1): 1-28.

[33] Hucker MJ, Bond IP, Haq S, Bleay S, Foreman A. Influence of manufacturing parameters on the tensile strengths of hollow and solid glass fibres. Journal of Materials Science 2002; 37(2): 309–315.